

A. Bossio¹, M. Montuori², F. Bellucci³,
G.P. Lignola⁴, A. Prota⁵, E. Cosenza⁶, G. Manfredir⁷

Indirect measure of corrosion level based on crack opening Pośrednia miara stopnia korozji bazująca na rozwarciu rysy

Keywords: RC structures, Corrosion, Assessment, Crack width, Design charts, Non Destructive Tests

Słowa kluczowe: konstrukcje żelbetowe, korozja, oszacowanie, szerokość rysy, nomogramy, testy nieniszczące

1. INTRODUCTION

When performing a static strengthening of the historic buildings, the most important issue is to respect existing materials and geometry. Therefore, the design proposal must include minimum of disruption and should be based on a demonstrated need. Because of historic importance of structures it is necessary that the solution is closely related to the diagnostic conclusions obtained from an accurate analysis of the structural members and materials. The most common analyses focus on feasible loads and static or dynamic behavior of structures. The formulation of a restoration design needs information about the geometry of the structure, the loads and the characteristics of the materials. The removal of several samples to be submitted to laboratory destructive tests could solve the problem, but this kind of approach could be expensive, or impossible to perform when structures have historical importance which prohibits any damage, even for diagnostic purpose. So it is necessary to adopt Non Destructive Tests (NDT) techniques.

The aim of this work is to correlate external crack widths, related to corrosion process only in Reinforced Concrete (RC) members, to bar cross sectional area reduction, focusing on numerical modeling. Corrosion process, presenting oxide volumetric expansion, leads to external cracks. The paper shows how, starting from external crack width, due to corrosion, it is possible to estimate the value of bar section lost due to corrosion and, consequently, the residual value of the load-bearing capacity of the structure.

Two different models have been considered. The first one represents an external (corner) bar and the other one represents an internal bar. Considering the two models, the approaches, based on Finite Element Method (FEM) results, give simple

formulations about relationship between external crack widths, w_c , and corrosion penetration, x . Each model has two correlations: a refined one and a simple one.

2. FEM ANALYSIS

To simulate old structures affected by corrosion crack opening, more than 200 FEM analyses were performed considering the variability of concrete cover, c_c , bar radius, R_0 , and concrete elastic modulus, E_c . A displacement was imposed to concrete along the bar perimeter to simulate oxide expansion and the crack opening on the external surface of concrete cover was recorded. FEM analyses have been performed using the TNO DIANA 9.4 code. Concrete is assumed elastic in compression and in tension, deformability of steel and oxide is neglected. Figure 1 shows main geometric parameters investigated by means of FEM analyses in order to simulate internal bars (Fig. 1a) and external bars (Fig. 1b), i.e. close to corners of cross sections.

2.1. Internal bar model

In order to simulate internal reinforcement bars, more than about 100 FEM analyses were performed. Three different values of bar radius, R_0 , (namely 5, 8 and 10 mm) and concrete cover, c_c , (namely 10, 30 and 50 mm) were considered. Results have been related to b_i , defined as internal distance (in the range 70 to 260 mm) between two consecutive bars, and potentially between two cracks, from a practitioner's point of view.

From a numerical point of view, boundary conditions for the FEM are given by a symmetry axis in the middle of the bar inside concrete core, a free edge along crack opening and

¹ PhD Candidate, University of Naples "Federico II" – DIMP, antonio.bossio@unina.it

² Associate researcher, University of Naples "Federico II" – DIMP, mamontuori@unina.it

³ Full professor, University of Naples "Federico II" – DIMP, bellucci@unina.it

⁴ Assistant professor, University of Naples "Federico II" – DIST, glignola@unina.it

⁵ Associate professor, University of Naples "Federico II" – DIST, aprota@unina.it

⁶ Full professor, University of Naples "Federico II" – DIST, cosenza@unina.it

⁷ Full professor, University of Naples "Federico II" – DIST, gamanfre@unina.it

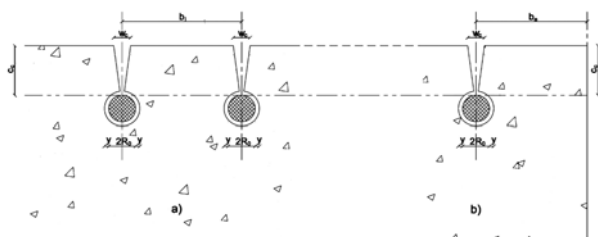


Fig. 1 geometric parameters of FEM analyses: a) internal bar, b) external bar

another symmetry constraint in between two consecutive bars. Figures 2a and 2b show numerical deformed configuration after displacement, y , of bar perimeter. It is noticed that higher bar diameters, $2 \cdot R_0$, or lower concrete covers, c_c , (Fig. 2a) yield to higher concrete cover displacement and crack width is increasing moving outward.

Conversely a higher concrete cover provides lower crack openings, w_c , and widths are decreasing moving outward.

In this way the ratio between w_c and y was related (Fig. 3) to two main parameters: concrete cover (marker shape and color), c_c , and b_i , while dependency on bar diameter (marker size) was negligible and there was no dependency on elastic modulus of concrete.

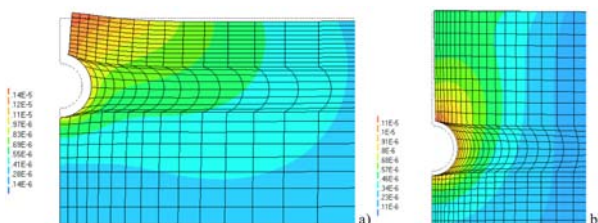


Fig. 2 FEM deformed shape: a) $c_c = 10 \text{ mm} - R_0 = 5 \text{ mm} - b_i = 125 \text{ mm}$, b) $c_c = 50 \text{ mm} - R_0 = 10 \text{ mm} - b_i = 80 \text{ mm}$

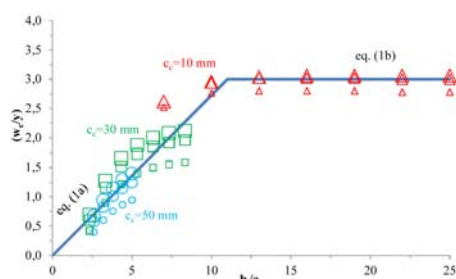


Fig. 3 Internal bar model. FEM results and best fitting curve – simple correlation

Equations(1a-b)represent the best fitting of numerical values of the ratios w_c/y :

$$\frac{w_c}{y} = \begin{cases} \frac{3}{11} \frac{b_i}{c_c}, & \text{if } b_i \leq 11c_c \\ 3.0, & \text{if } b_i > 11c_c \end{cases} \quad (1)$$

Figure 3 presents simple evaluation of w_c/y ratios calculated by equations (1a-b). However a more refined correlation was found in the form (Fig. 4a):

$$\frac{w_c}{y} = A \cdot \ln(b_i) + B \quad (2)$$

where both A and B coefficients depend on concrete cover values, c_c , and a linear interpolation (Fig. 4b) provides satisfactory

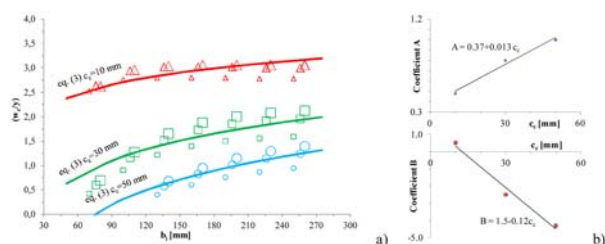


Fig. 4 Internal bar model. FEM results and fitting curves related to b_i and c_c

agreement for them. FEM results are, in fact, clearly grouped according to the concrete cover values, c_c , (and dependency on bar diameter is negligible). Fitting curves, considering variability of c_c and b_i , can then be expressed by equation (3) as reported in Fig. 4a:

$$\frac{w_c}{y} = (0.37 + 0.013 \cdot c_c) \cdot \ln(b_i) + 1.5 - 0.12 \cdot c_c \quad (3)$$

2.2. External bar model

As well as for previous model, about 100 FEM analyses were performed in order to simulate external reinforcement bars, considering the same parameters, with the only exception of b_e , ranging between 35 and 130 mm. Furthermore, in this case, it is implicitly assumed that $c_c \leq b_e$, otherwise a crack opening can be expected on the orthogonal side (due to minor resistance).

From a numerical point of view, the same boundary conditions as before were considered, but in this case, instead of the axis of symmetry in between two consecutive bars, there is the free edge of the lateral concrete surface. Figures 5a and 5b show the deformed shape in the case of external bars. In this case it is noticed that the higher are bar diameters, $2 \cdot R_0$, or the lower are concrete covers, c_c , (Fig. 5a) then the higher is crack opening. In this case concrete cracks are usually increasing moving in the outward direction. Again the ratio w_c/y was related (Fig. 6) to b_e , while dependency on c_c (marker shape and color) and bar diameter (marker size) was negligible; again there was no dependency on Young's modulus of concrete, E_c .

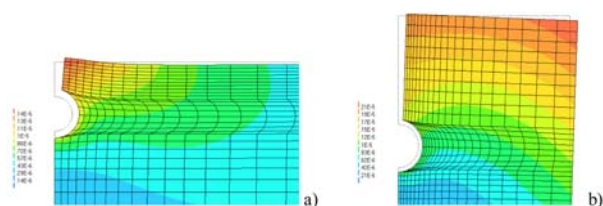


Fig. 5 FEM deformed shape: a) $c_c = 10 \text{ mm} - R_0 = 5 \text{ mm} - b_e = 125 \text{ mm}$, b) $c_c = 50 \text{ mm} - R_0 = 10 \text{ mm} - b_e = 80 \text{ mm}$

A simple correlation was found according to figure 6, neglecting also the dependency on concrete cover, according to equation (4) related to b_e only:

$$\frac{w_c/y}{b_e} = \frac{1981}{50} \cdot b_e^{-1.556} \rightarrow \frac{w_c}{y} = \frac{1981}{50} \cdot b_e^{-0.556} \quad (4)$$

In order to find a more refined correlation, FEM results were grouped according to the concrete cover values, c_c , (for every considered bar diameter) and plotted in figure 7. A more refined correlation was found in the form:

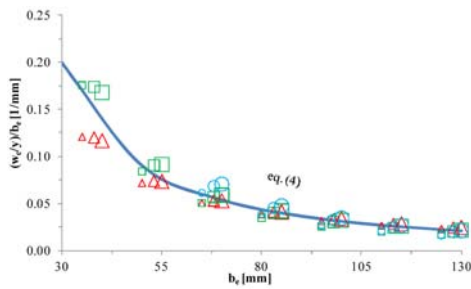


Fig. 6 External bar model. FEM results and best fitting curve – simple correlation

$$\frac{w_c/y}{c_c} = C \cdot b_e^D \quad (5)$$

where both C and D coefficients depend on concrete cover values, c_c (Fig. 7b). A linear interpolation provides satisfactory agreement for C, while logarithmic interpolation provides best results for D. Fitting curves, considering variability of c_c and b_e , can then be expressed by equation (6) as reported in Fig. 7a:

$$\frac{w_c}{y} = \left(\frac{34 + 3.6 \cdot c_c}{50} \right) \cdot c_c \cdot b_e^{(0.6 - 0.39 \cdot \ln c_c)} \quad (6)$$

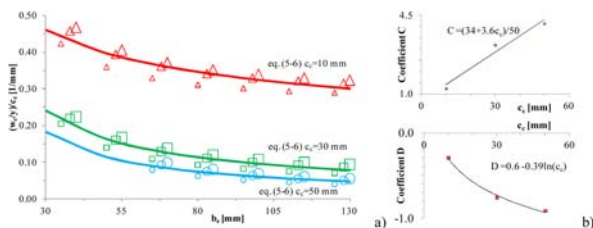


Fig. 7 External bar model. FEM results and fitting curves related to b_e and c_c

3. CORROSION PENETRATION AND OXIDE EXPANSION

Previous models gave a correlation between w_c/y ratio and b_e or b_i , depending on bar position, related to concrete cover, c_c , and neglecting bar radius, R_0 . In reality, corrosion penetration, more than bar expansion (due to oxide production), is of interest. In fact such parameter allows to evaluate residual strength capacity of internal reinforcement, to correlate corrosion rate with actual penetration and thus to estimate corrosion initiation or future corrosion evolution with time. Strength capacity, for instance, is related to cross section of bars. Presented models give the w_c value related to bar expansion, y , however it is still possible to relate y to corrosion penetration, x , (Fig. 8a) by means of volumetric expansion coefficient, n , related to the oxide generated by corrosion process. Such coefficient usually ranges between 2 and 6 [1]. A simple continuity equation [2], allows to relate x and y :

$$\pi \cdot [(R_0 + y)^2 - (R_0 - x)^2] = n \cdot \pi \cdot [R_0^2 - (R_0 - x)^2] \quad (7)$$

hence to evaluate directly y values:

$$y = \sqrt{(1 - n) \cdot (R_0 - x)^2 + n \cdot R_0^2} - R_0 \quad (8)$$

Equation (7) represents the continuity equation where the volume of produced oxide $\pi \cdot [(R_0 + y)^2 - (R_0 - x)^2]$

is equal to n times the volume of bar consumed $\pi \cdot [R_0^2 - (R_0 - x)^2]$.

A further simplification is given by normalization of y and x with respect to R_0 , in fact equation 8 becomes:

$$\frac{y}{R_0} = \sqrt{(1 - n) \cdot \left(1 - \frac{x}{R_0}\right)^2 + n} - 1 \quad (9)$$

Typical values of x/R_0 are usually lower than 0.2 (this means a corrosion penetration of about 2 mm in radial direction on a bar having $R_0 = 10$ mm, or in other words a heavy reduction of cross section of about 35%). The curve given by equation (9) can be easily approximated by a linear equation, thus by a simple $y = F \cdot x$ relationship. This approximation simplifies the correlation of x with w_c .

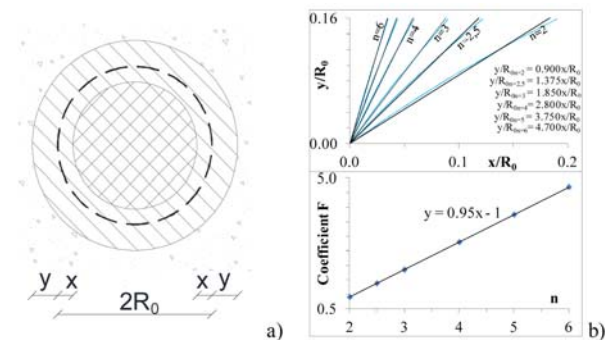


Fig. 8 a) Geometric scheme of oxide expansion; b) y/R_0 vs. x/R_0 and fitting curve

In figure 8b variability of n coefficient is considered. It is observed that the higher is n , the greater is oxide expansion, y/R_0 , ratio for a given corrosion penetration, x/R_0 , ratio. A simplified linear relation between x and y , according to fitting curves reported in figure 8b) is given by equation (10), neglecting dependency on R_0 :

$$\frac{y}{R_0} \cong (0.95 \cdot n - 1) \cdot \frac{x}{R_0} \rightarrow x \cong \frac{y}{(0.95 \cdot n - 1)} \quad (10)$$

4. DESIGN CHARTS

Design charts can be easily provided, according to refined models – i.e. equations (3) and (6) – to correlate crack opening on concrete surface and oxide expansion. The dependency is limited only to concrete cover, c_c , and crack distance, b_i from another crack or b_e from cross section corner (respectively for internal and external bars). Figure 9 shows w_c/y ratio vs. b_i , considering variability of c_c . It is noticed that w_c/y ratio grows as b_i grows. Figure 10 shows w_c/y ratio vs. b_e , considering variability of c_c . In this case w_c/y ratio seems to be less dependent on concrete cover, c_c . These design charts are based on two parameters, concrete cover, c_c , and crack distance, b_i or b_e both of them are almost easily assessable.

Even if simplified equation (10) suggests that, given a volumetric expansion coefficient, n , of oxide, there is no strict dependency on bar radius, R_0 ; refined equation (8), accounting for R_0 , shows that knowledge of bar radius is less relevant than knowledge of concrete cover and crack distance b_i or b_e . In fact figures 11 and 12 show directly the relation between w_c and x , by means of refined models (equations (3) or (6) to evaluate w_c/y and equation (7) to evaluate x). In this evaluation

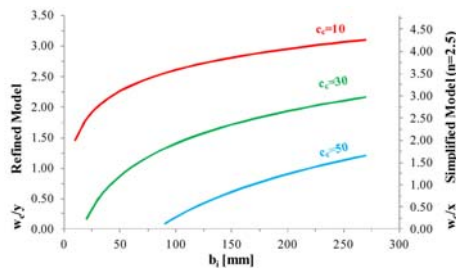


Fig. 9 Design chart: external bar – w_c/y ratio or w_c/x (y/x simplified and $n = 2.5$) vs. b_i

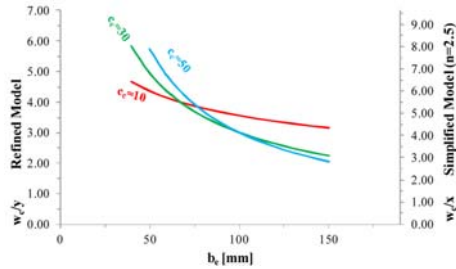


Fig. 10 Design chart: external bar – w_c/y ratio or w_c/x (y/x simplified and $n = 2.5$) vs. b_e

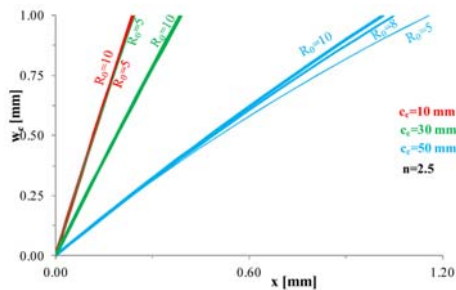


Fig. 11 Direct evaluation w_c vs. x in case of internal bar (refined model and $b_i = 170$ mm)

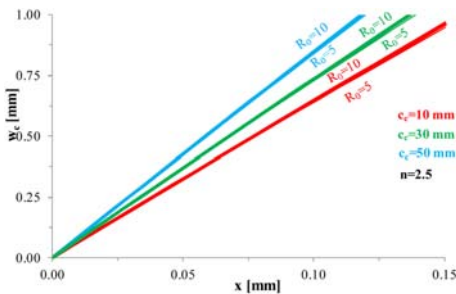


Fig. 12 Direct evaluation w_c vs. x in case of external bar (refined model and $b_e = 50$ mm)

a low value for n is assumed, i.e. $n = 2.5$, on safe side (because it leads to higher corrosion penetrations). This plot confirms that dependency on R_0 is almost negligible.

It is an important outcome, in fact, bar radius is not easily assessable (e.g. especially if it is not allowed to remove concrete cover, as in a cultural heritage structure).

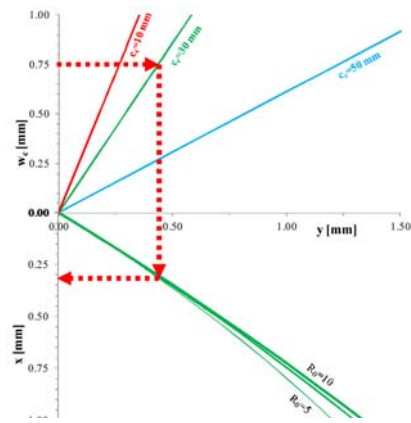


Fig. 13 Illustrative example: w_c-x in the case of $n = 2.5$ and $b_i = 150$ mm (Eqs. 3+8)

4.1. Illustrative example

Given, for instance, a series of cracks on the external side of a RC column, spacing each other about $b_i = 150$ mm, and evaluating a concrete cover $c_c = 30$ mm (but the same can be repeated for other concrete covers, e.g. 10 mm and 50 mm, respectively), a value of w_c/y ratio is found on Design Chart, figure 9, equal to 1.7 (2.8 or 0.6 for other covers, respectively). Then the estimation of internal bar radius allows to move from oxide expansion, y , to corrosion penetration, x . This is illustrated in figure 11 where, given $w_c = 0.750$ mm and $c_c = 30$ mm, y is equal to 0.440 mm and finally, considering a D16 bar, corrosion penetration is $x = 0.307$ mm. This for instance leads to a reduction of bar cross section of about 8%, however in the assessment of the structure the degradation of the cracked concrete should also be included.

The same example is repeated in Table 1, for a given crack opening of $750 \mu\text{m}$, reporting the predictions of corrosion penetration, x , according to different methods, namely FEM simulation, fully refined model (i.e. previous description) based on refined w_c/y model (i.e. equation 3) and refined y/x model (i.e. equation 8), and other combinations of w_c/y (i.e. equations 1 or 3) and y/x models (i.e. equations 8 or 10).

Table 1 reports also, as subscript, the percentage variation with respect to FEM. Even if the maximum scatter is not always negligible, in authors' opinion this is fully reasonable if compared to uncertainties in the measurement of crack opening and the development of corrosion process. For instance



Fig. 14 Typical onsite assessment of crack opening and 25X high definition photo enlargement

Table 1 Corrosion penetration x (in μm) according to different models ($n = 2.5$; $b_i = 150$ mm and $w_c = 750 \mu\text{m}$)

c_c [mm] R_0 [mm]	10			30			50		
	5	8	10	5	8	10	5	8	10
FEM+Eq. 8	187	170	168	412	324	301	1215	810	712
Eqs. 3+8	186 _{-1%}	183 _{+8%}	182 _{+8%}	316 _{-23%}	307 _{-5%}	303 _{+1%}	1024 _{-16%}	936 _{+16%}	910 _{+28%}
Eqs. 3+10	194 _{+4%}	194 _{+14%}	194 _{+15%}	319 _{-23%}	319 _{-2%}	319 _{+6%}	893 _{-27%}	893 _{+10%}	893 _{+25%}
Eqs. 1+8	174 _{-7%}	171 _{+1%}	170 _{-1%}	403 _{-2%}	389 _{+20%}	384 _{+28%}	719 _{-41%}	675 _{-17%}	661 _{-7%}
Eqs. 1+10	182 _{-3%}	182 _{+7%}	182 _{+8%}	400 _{-3%}	400 _{+23%}	400 _{+33%}	667 _{-45%}	667 _{-18%}	667 _{-6%}

a refined measure on a high definition 25X enlargement of crack opening, as in the case depicted in figure 14, is out of the ordinary during onsite assessment, being field precision in the order of tenth or, at best, hundredth of millimeter.

5. CONCLUSIONS

Analytical correlations between crack opening, as it can be measured on concrete surface of corroded RC structural members, and corrosion penetration on internal reinforcement bars are provided. Different sets of interpolating equations are provided: simple ones, for fast onsite estimations, and refined ones for precise assessments. A wide range of values for main geometrical parameters was adopted to cover most common RC member configurations. The development of the equa-

tions takes into account the availability of input parameters. The influence of uncertainty on parameters, which are difficult to assess, is discussed; namely the bar diameter is the most difficult to evaluate, especially in cultural heritage structures, but its influence is practically negligible. Then the influence of concrete cover is discussed; its thickness is still not always easily available, and for this reason some simplified interpolations were developed to neglect its value. Finally, external dimensions of crack spacing or distance from a free edge of concrete members, easily quantifiable, are the driving parameters of the proposed models. A maximum scatter, lower than about 30%, was found for refined models; further onsite validation is needed, nevertheless it is considered reasonable because of ordinary uncertainties in crack opening measurements onsite and in corrosion process, in general.

REFERENCES

- [1] Pedferri, P., Bertolini, L. (2000). *La durabilità del calcestruzzo armato*, McGraw-Hill, Milano, Italy (in Italian).
- [2] Bossio, A. Montuori, M. Bellucci, F. Lignola, G.P. Prota, A. Cosenza, E. & Manfredi, G. (2011) Analytical modeling of reinforcement corrosion effects on RC members degradation. In: *2nd Workshop: The new boundaries of structural concrete*. Imready, Ancona, Italy: 205-213.

Abstract

Reinforced concrete (RC) is a widely used material since about 100 years. The early degradation of RC structures has led to intervene on them. Main causes of degradation are carbonation, chlorides and sulphides attacks. Even if diffusion of RC structures is quite recent, however historical and cultural heritage constructions are also made of RC. To preserve the historic value of such structures could require minimally invasive measures aimed at long-term safeguarding, if they are well designed; but it is important to evaluate material characteristics. For this purpose it is necessary to use non destructive tests (NDT) to evaluate the level of degradation reached by the materials composing the structures. Main electrochemical NDT are measurement of corrosion rate and open circuit potential. The use of such techniques requires the removal of small portions of concrete cover only.

They, indirectly, allow the value of corrosion penetration to be evaluated.

Previous studies provided analytical models to assess crack initiation and propagation according to different values of concrete strength, concrete cover, bar diameter and type of aggregates. Such models better perform for new buildings because historic structures are usually expected to present a visible crack pattern. This paper presents another tool in the box of practitioners to assess and evaluate the vulnerability of existing structures. In particular proposed model provides bar reduction in terms of diameter or cross sectional area, depending on actual crack opening. Outputs of the paper are design charts providing direct correlation between crack width and steel reinforcement loss depending on few geometrical dimensions of RC elements.